



Experimental Characterization of Dimensional and Surface Alternation of Straight and Angular Cutting on Self-lubricating Composite: A Wire EDM Approach

A. Gnanavelbabu¹ · K. Rajkumar²

Received: 3 February 2020 / Accepted: 26 April 2020 / Published online: 12 May 2020
© King Fahd University of Petroleum & Minerals 2020

Abstract

Demands on better control over the kerf dimension deviation, surface roughness, and corner accuracy are now on the increase for the two-piece aluminum metal composite mold tools. In this investigation, straight and triangular profile cuts attempted with wire electrical discharge machining (WEDM) on the aluminum 6061 self-lubricating composite-reinforced boron carbide (5–15 vol%) and hexagonal boron nitride particles (10 vol% hBN) fabricated using a stir casting method. Rational video measurement showed an increase in B₄C particles reduces kerf width dimension deviation only at T_{ON} , T_{OFF} and gap voltage (V) parameters. Optical microscope measurement showed an increase in the corner area inaccuracy increases with both low and high pulse-on duration conditions caused by insufficient material removal and a high order of erosion, respectively. There was a large reduction in corner area inaccuracy with increasing wire feed rate. Surface characteristics were examined using a scanning electron microscope (SEM) and XRD to enable observation of the structural damages and recast layers. Composite with 5% boron carbide showed a re-deposition layer over the machined surface, whereas 15% boron carbide composite went through uneven erosion causing the formation of craters and pits on the cutting surface resulting in higher surface roughness.

Keywords Composite · Electric discharge · Solid lubricant · Erosion · Surface roughness · Kerf

1 Introduction

Aluminum alloy metal mold tools are found exclusive use in the production of seat foams, urethane panels, silicone patterns, and MRI instrument cover panels [1]. Aluminum alloy metal molds are preferred due to their efficient heat transfer and moderate mechanical strength. These molds are frequently subjected to wear and tear on mating surfaces, wear of edges and corners, and increase in the surface roughness. Demands for better dimension control over the corner accuracy and surface roughness are on the increase in two-piece metal mold tools. In order to improve the tribological performance of two-piece metal mold, aluminum metal matrix composite is designed with a combination of ceramic

reinforcement and solid lubricant particles. Harder ceramic reinforcement provides wear resistance to the metal matrix [2], whereas the soft lubricant produces an anti-friction layer on the mating surface which supports free sliding [3]. The presence of a solid lubricant also facilitates easy separation of two-piece mold after the completion of the manufacturing cycle without any score marking on the mating surfaces [4, 5].

Aluminum metal matrix composite (AMMC) made of an aluminum matrix reinforced with mono- or multiple ceramic particles. Particulate reinforcements are regularly used in carbides of various forms and borides for the improvement of AMMC properties [6–10]. Boron carbide has still opted as a ceramic reinforcement as it is next to diamond strength [11]. The hexagonal boron nitride (hBN) particles provide a self-lubrication property and can form a mechanically mixed layer with ceramic particles [12]. This reduces friction and rapid wear of the mating surface. A point to note is that a small hBN volume fraction in the metal matrix has a meager effect on the base material mechanical properties but beneficial for the tribology aspects [13–15]. The combination of

✉ K. Rajkumar
rajkumark@ssn.edu.in

¹ Department of Industrial Engineering, CEG Campus, Anna University, Chennai 600025, India

² Department of Mechanical Engineering, SSN College of Engineering, Chennai 600110, India



ceramic and solid lubricant particulate composite provides a self-lubricating metal matrix composite (SLMMC).

Manufacturing processes available for the fabrication of SLMMC-based mold tools are limited in number. The existence of harder reinforcement particles has a serious effect on surface finish and form accuracy [16], leading to the unsuitability of conventional machining. Unconventional wire electric discharge machining (WEDM) is a widely recognized process for making metal molds/dies with complex shapes irrespective of their mechanical characteristics [17, 18]. This process eventually produces a good surface finish with enhanced corner accuracy [19].

Previous studies focused on the WEDM machining behavior and process optimization of metal matrix composites. Shandilya et al. [20] have investigated the WEDM behavior of aluminum (AA6061)-SiC_p composite. Reinforced SiC composite subjected to severe thermal damage due to repeated discharge sparks, and it ended up with poor surface quality. Ekici et al. [21] evaluated the WEDM characteristics of hot-pressed Al/B₄C MMC. They observed the effect of every increment in B₄C volume fraction on the material removal rate (MRR) and surface finish. Ramesh et al. [22] have presented a detailed WEDM experimentation on the Al6061/SiC/B₄C_p hybrid MMC. They have also reported the significant effect of the surface roughness and MRR with the weight percentage of reinforcements. Pramanik and Little fair [23] proved that the presence of finer reinforcement particles in the MMC increases the WEDM cutting quality characteristics. Manna and Bhattacharyya [24] improved process competency by reducing wire breakage frequency and the high dielectric water flushing pressure. Yan et al. [25] showed the frequent prevention of wire damage through control of dielectric flushing rate and wire speed during the machining of Al (6061)-Al₂O_{3p} composite. Motorcu et al. [26] confirmed the presence of B₄C reinforcement in MMC directly affecting matrix melting and evaporation phenomena.

The common variables of WEDM are mainly affecting cutting dimensionality of various materials, namely pulse current, time-on and off duration, gap voltage, wire feed, and insulating fluid type and pressure. Kandpal et al. [27] confirmed the increasing of MRR and surface roughness (SR) of WEDM processed AA6061/10%Al₂O₃ MMC with pulse-on duration and pulse current. Mohinder Pal Garg and Anand Sharma [28] analyzed the kerf dimensional deviation produced by the WEDM process on the ZrSiO_{4p}/AA6063 composite. They have found that pulse-on time and wire feed rate are significant process parameters. In solitary pass WEDM cutting, path and process parameters modification approaches implemented for the reduction of corner inaccuracy of AISI D2 tool steel [29]. Selvakumar et al. [30] have also proposed the improvement of corner accuracy by parameter modification strategy for the Monel

alloy cutting. They observed a larger wire lag due to a sharp corner angle, heavy thickness, and different nozzle height. These are affecting corner dimensions. The corner error has been reduced by subsequent trim-cut operation [31]; on the other hand, it leads to time and cost of machining.

Previous studies have focused on the WEDM of MMCs with mono- or hybrid ceramic reinforcement particles and reported geometrical kerf and dimensional shift for straight slit cut. Moreover, researchers vastly studied corner area accuracy of steel dies, which is the most important quality characteristic. WEDM characteristics and measurement of corner accuracy of aluminum self-lubricating composite mold tool still require a comprehensive study.

This research investigation consists of a comprehensive experimental analysis on the WEDM of self-lubricity composite and measurement of kerf dimension deviation, surface characteristics, and corner area inaccuracy using rational video, Talysurf CCI Lite, and optical measurement systems.

2 Experimental Procedures

2.1 Materials, Fabrication, and Microstructure Analysis of Self-Lubricating Composite

Aluminum 6061 series self-lubricity composite made with 5%, 10%, and 15 vol% boron carbide (B₄C) and hBN of 10 vol% particles. A two-step liquid metallurgy route selected for the fabrication of the aluminum hybrid MMC [32]. The size of the hBN particle was 5 μm, and that of the B₄C reinforcement particle size was 10–25 μm. Aluminum 6061 material was melted in a graphite crucible using an electrical resistance furnace. The heating process was done gradually to reach 800 °C temperature. The flux charged over the melt and zirconia-coated stainless steel was stirred vigorously with a rotational speed of 500 RPM. A vertex was formed as a result of continuous stirring. This vertex helps in getting a uniform dispersion of reinforcement particles in the molten metal. B₄C and hBN particles were preheated earlier for improving their wettability with liquid metal. Composite melt was poured into rectangular mild steel die for preparing self-lubricating MMC of dimension 100 × 100 × 10 mm.

Self-lubricating composite (SLC) fabricated from the aluminum matrix, ceramic and solid lubricant particles. This composite has a self-lubricating property. Table 1 shows the composite designation and its volume proportion of B₄C and hBN particles in the self-lubricating composite. SEM images of SLC 5, SLC 10, and SLC 15 are shown in Fig. 1a–c, confirming the fair distribution of reinforced particles in the composite microstructures. Figure 1d shows the energy-dispersive spectrum (EDS) revealing the intensity peaks of aluminum alloying elements, B₄C, and hBN of the fabricated composite.



Table 1 Composition of fabricated composites

Self-lubricity composites designation	B ₄ C (vol%)	hBN (vol%)	Aluminum
SLC 5	5%	10%	Balance
SLC 10	10%	10%	Balance
SLC 15	15%	10%	Balance

2.2 Mechanical Properties

Hardness of the fabricated composites tested using a Vickers hardness machine with an indentation load of 250 kgf, following the ASTM E92 standard. Five indentations were made for each composite sample and reported with standard deviation. The tensile strength of the prepared composites found using a universal testing machine with a cross-head velocity of 2 mm/min following the ASTM E9 standard. The gauge length, width, and thickness of the sample were 25 mm, 4 mm, and 3 mm, respectively. The tensile strength of the composite had a measurement of five readings with standard deviation.

2.3 Straight and Triangular Profile Cutting

In this research work, wire electrical discharge machine (4-axis CNC Eco-cut) was used for cutting composites. A zinc-coated brass wire of 0.25 mm diameter was used as a negative electrode terminal, and fabricated composite was a positive terminal. Demineralized water was a dielectric medium that helped to flush out the debris generated during machining. Two types of cuts separately made on the composite materials, i.e., straight cut and triangular profile cut with the same process parameters.

The kerf width dimensional deviation and surface roughness of the straight cut were measured, and the corner inaccuracy of the triangular cut was also measured. Effective process parameters, namely pulse time-on (T_{ON}) and off duration (T_{OFF}), gap voltage (V), and wire feed (f), are selected in line with reference [33]. Table 2 shows the process parameters used for the WEDM of composite.

2.4 Measurement of Dimensional Deviation and Surface Characteristic

The deviation of the kerf width dimension from the straight cut was measured using a rational video measurement system (VMS-2010 F) and reported by averaging the kerf width of the top and the bottom. The images were taken by a

Fig. 1 Microstructure and EDS of fabricated composites. **a** SLC 5. **b** SLC 10. **c** SLC 15. **d** Typical EDS profile

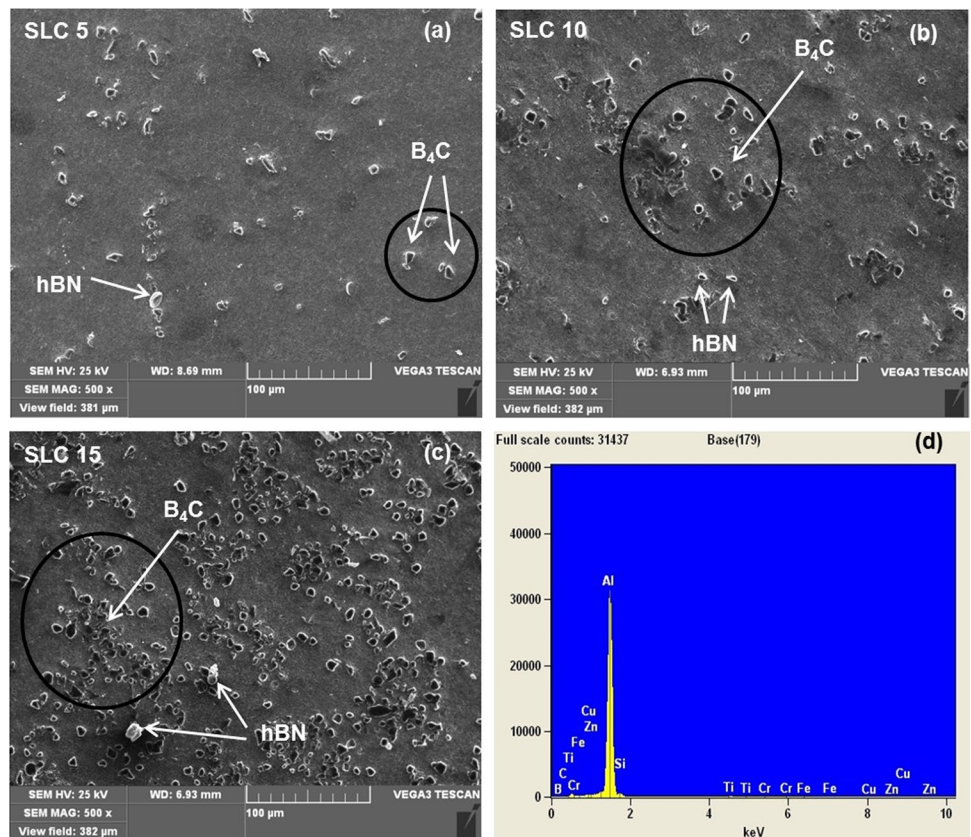
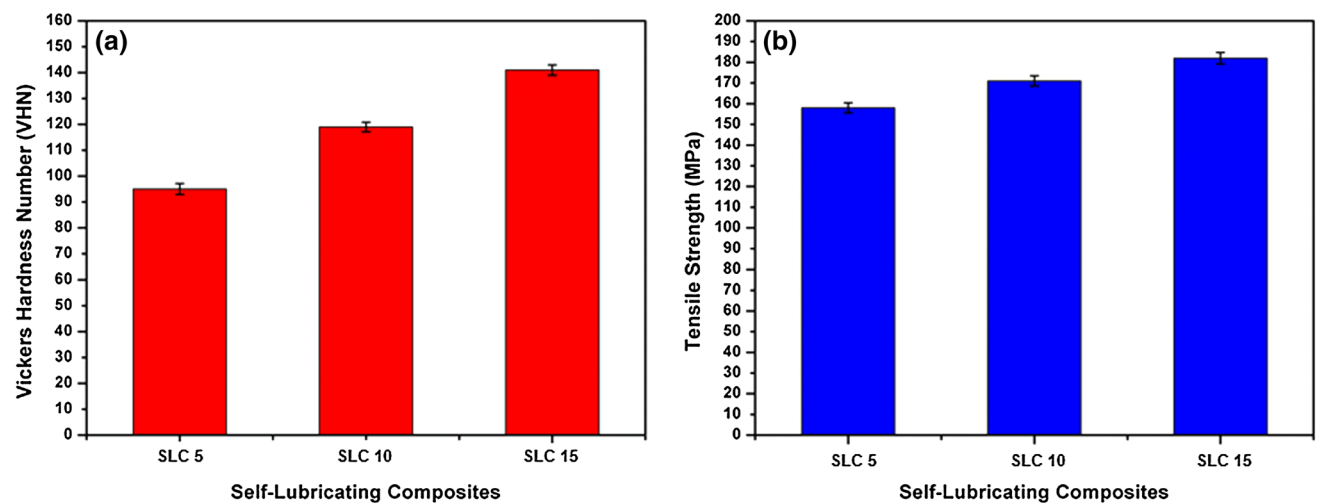
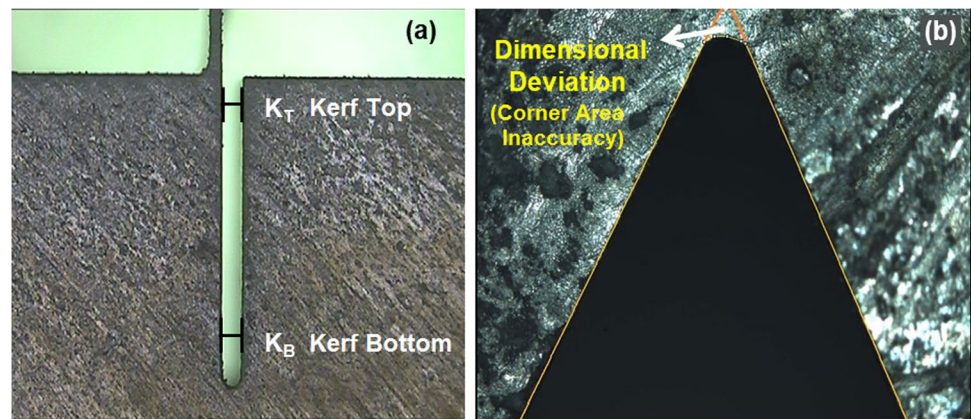


Table 2 Process parameters of WEDM

Parameters	Range of operation
Wire diameter	0.25 mm
Wire type	Zinc-coated brass
Dielectric fluid	Demineralized water
Pulse current	25 A
Pulse-on time (T_{ON})	2, 3, 4, 5, 6 μ s
Pulse-off time (T_{OFF})	6, 7, 8, 9, 10 μ s
Wire feed (F)	5, 6, 7, 8, 9 mm/min
Gap voltage (V)	45, 50, 55, 60, 65 V

CCD color camera with 2D/3D measurement software. The deviations of the dimension of the corner area by triangular profile cut were also measured using an optical microscope with image processing. Figure 2a, b shows the typical VMS image of the kerf width of the straight cut and optical image of the corner area of triangular cut.

Fig. 2 Profile geometry. **a** Typical kerf width. **b** Corner area**Fig. 3** Mechanical properties of fabricated composites. **a** Hardness. **b** Tensile strength

Surface roughness (R_a in μ m) from the straight cut was measured using Talysurf CCI lite. The cutoff length of 0.8 mm and a vertical resolution of 0.01 nm for each measurement set as constant. Surface roughness is measured along the thickness direction at three equally spaced locations, and the average value was reported.

3 Results and Discussion

3.1 Hardness and Tensile Strength Analysis

Figure 3a depicts the hardness of the fabricated composites. It shows the increase in the hardness of the fabricated composites caused by the B_4C particles when considering a constant hBN volume fraction. Generally, the addition of ceramic reinforcement particles improves the hardness of the matrix. This could be due to the increased strain energy of the matrix at the interface of reinforcement particles [34].

Figure 3b shows the tensile strength variations seen in SLC 5, SLC 10, and SLC 15 composites. An increase in the tensile strength of the aluminum matrix caused by transferring the load to the reinforcement B4C particles is seen [35]. This is also due to the disparity of thermal expansion of boron carbide and aluminum matrix at the interface causes a larger increase in dislocation density [36]. This improves the deformation resistance ability of the composite.

3.2 Kerf Width Measurement Analysis

The steady increase in kerf width dimension with pulse-on duration is shown in Fig. 4. The SLC 5 composite shows a larger kerf width compared to other composites. A narrow difference in kerf width dimension between SLC 10 and SLC 15 composites is observed. It is well known that the addition of ceramic reinforcement particles reduces the electrical conductivity of the composite which might have an effect on erosion characteristics. The narrowest kerf width dimension was achieved for the SLC 15 composite. During SLC 5 composite machining, however, no wire breakage was observed. Wire breakage at high pulse-on duration and high volume fraction of reinforcement particles [37] were also observed. It is clearly evident that B₄C ceramic particle aggravate problems in composite machining were seen. A high melting point leading to the requirements of requires high thermal energy per unit volume for hBN and B₄C to melt and vaporize the composite material. Therefore, the kerf width was narrower for the SLC 10 and SLC 15 composites.

Pulse-off duration (T_{OFF}) is the crucial parameter in WEDM that regenerates the insulation between the working gap and deionized water for consecutive pulse discharges. Normally, the machining rate is low for a longer pulse-off duration. The kerf width of composites was notably reduced

with increasing pulse-off duration as shown in Fig. 5. Lee and Li [38] found that the EDM machining rate of tungsten carbide reduced with the increase in pulse-off time.

The frequency of consecutive energy pulse is high at a shorter pulse-off generation. Ultimately, it produces craters and microcracks on the cutting surface. These defects clearly are shown in Fig. 6a. Besides, the probability of wire damage is also significantly high. This further affects the dimension and quality of the machined surface [39].

There is an insufficiency in the dislodging of B₄C and hBN particles at a longer pulse-off time. The resulting lower kerf width is observed. On the other hand, erosion of the aluminum matrix continued around the reinforcement particles, exposing the reinforcement particles to the cutting surface, as shown in Fig. 6b.

Referring to Fig. 5, the increase in kerf width is observed when the pulse-off duration exceeds 8 μs. A longer pulse-off duration helps the dielectric medium flushing of the debris and disintegration of B₄C and hBN particles between the electrodes gap, paving the way for fresh aluminum matrix erosion.

Figure 7 depicts the wire feed rate on the kerf width dimension variation in the composites. The experimental results revealed a reduction in the kerf width caused by the wire feed rate. At slow wire feeding with reference to the work material, prolonged discharge energy at the same place often increases the material removal and also dislodges B₄C and hBN particles producing a wider kerf width. A small volume of metal matrix supports B₄C and hBN particles at higher reinforcement volume fraction. The dislodging of reinforcement particles is more severe. Eventually, it leads to a larger-dimensional inaccuracy.

The wire electrode is seen steadily moving through the machining path at a higher wire feed rate. At this feed rate, wire traveling across the workpiece continued with very

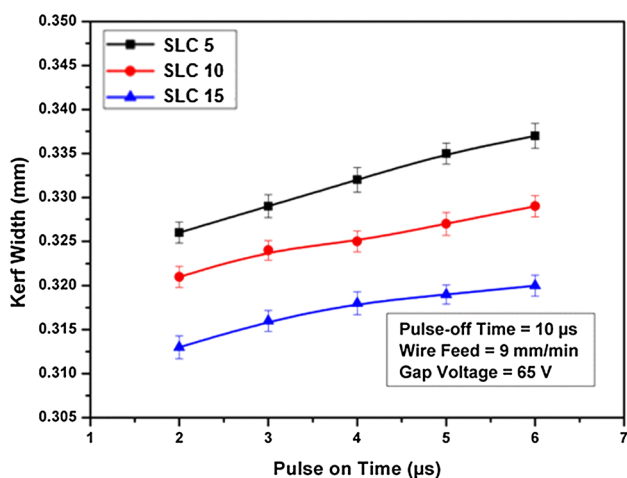


Fig. 4 Analysis of kerf width by pulse-on time

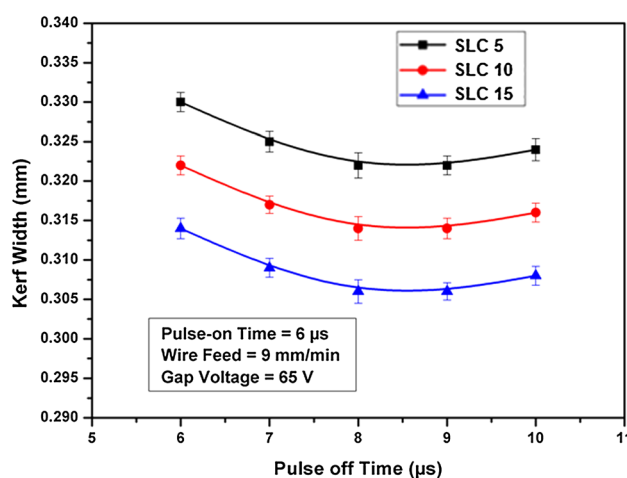


Fig. 5 Analysis of kerf width by pulse-off time

Fig. 6 SEM images of machined composites at different pulse-off times

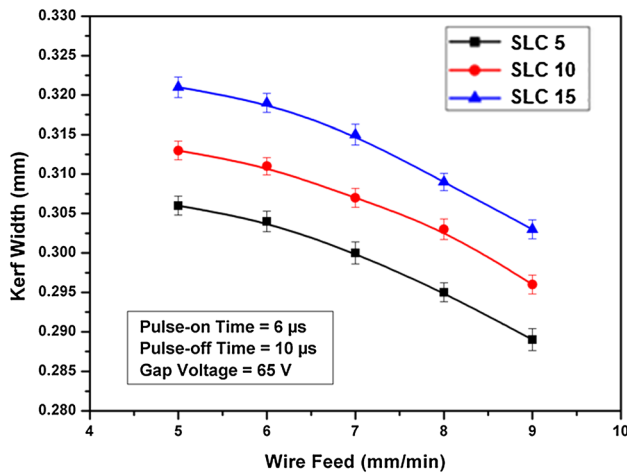
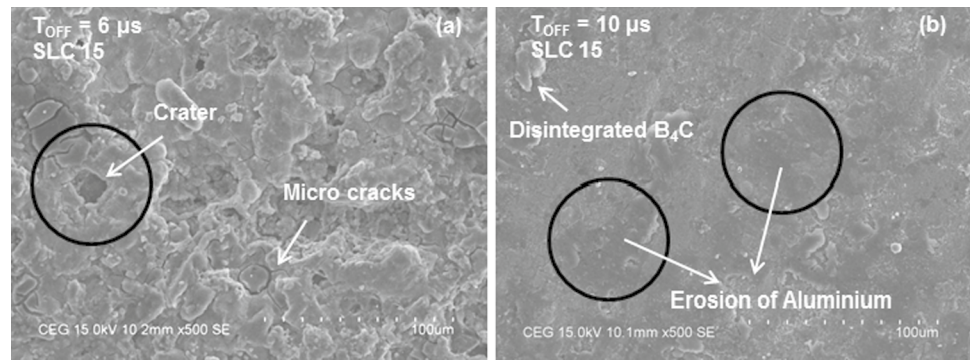


Fig. 7 Analysis of kerf width by wire feed

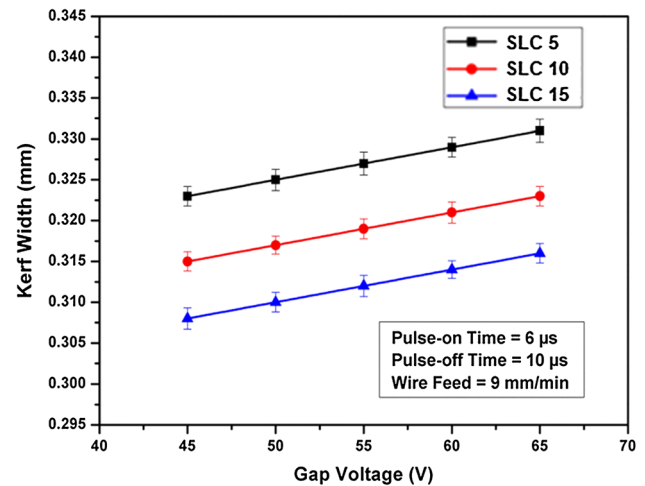


Fig. 8 Analysis of kerf width by gap voltage

small wear. This was due to the wire itself fasting before reaching the discharge spark. This resulted in an almost constant wire diameter for the entire machining period. Therefore, the kerf width dimension was as good as in the higher wire feed rate. A considerable wire electrode wear was due to the repeat spark discharges at a lower feed rate. There was a gradual decrease in the wire diameter throughout the machining period [40], affecting the kerf width dimension.

Figure 8 reveals the effect of gap voltage on the kerf width dimension variations in the machined composites. Gap voltage usually causes an increase in the discharge current intensity. At a higher gap voltage, there was a rapid erosion of aluminum metal due to an increase in the kerf width dimension caused by high spark energy. But erosion was lower with an increase in the volume fraction of the reinforcement particles. Apparently, the reinforcement particle decreased the kerf width dimension. During machining, a majority of the debris along with the dislodged reinforcement particles could obstruct their inter-electrode gap. This affected material removal and hence needed effective flushing [16].

3.3 Surface Roughness Analysis

Figure 9 shows the surface roughness of machined composites as a function of the pulse-on duration. SLC 10 composite shows the finest surface. In SLC 5 composite, the aluminum metal volume relatively high with larger metal erosion was seen. This turned into a re-deposition layer over the machined surface with many craters and pits resulting in poor surface finish. For SLC 15, the high reinforcement particles caused the wandering of the electric sparks over the surface. This caused uneven machining on the cutting surface, leading to the surface roughness of SLC 5 and SLC 15 getting poor. In the case of SLC 10, the presence of a balanced amount of matrix and reinforcements reduced the effects. This results in a reduction of thermal energy induced defects on the machined surface [22], decreasing surface undulation.

Figure 10 shows the SEM images of the machined composites at different T_{ON} . Spark discharges energy at shorter pulse-on duration inducing micro-cracks on the machining surface, as shown in Fig. 10a, b. Discharge energy for a longer duration produces deep and wider craters, as shown

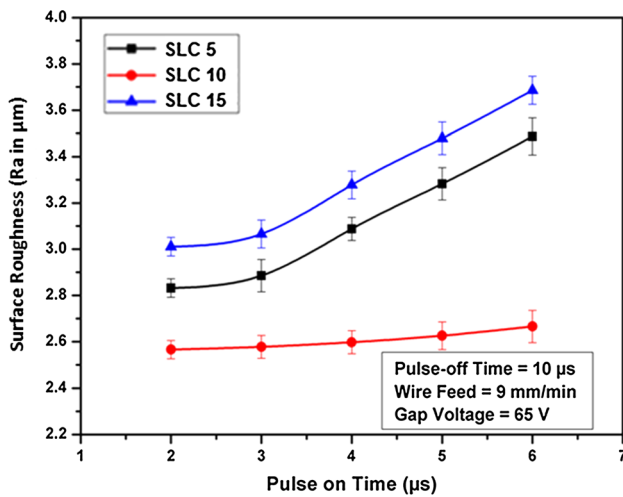


Fig. 9 Analysis of surface roughness by pulse-on time

in Fig. 10c, d. The discharge energy was more with high peak current, for a longer duration of the pulse, which increases the surface roughness of composite material machined surface [41, 42]. SLC 15 composite also shows a poor machined surface with rough patches, fissures, and craters marks, as shown in Fig. 10d.

Another result of the longer pulse-on duration was the reinforcement particles getting mixed within the re-deposited layer. This confirmed through a comparison of X-ray

diffraction peaks of the re-deposition layer at a shorter and longer pulse-on time, as shown in Fig. 11a, b.

An increase in reinforcement particles reduced the thickness of the re-deposition layer shown in Fig. 12a–c. Further, an edge melting was observed at SLC 15 composite that leads to burr formation, as shown in Fig. 12d.

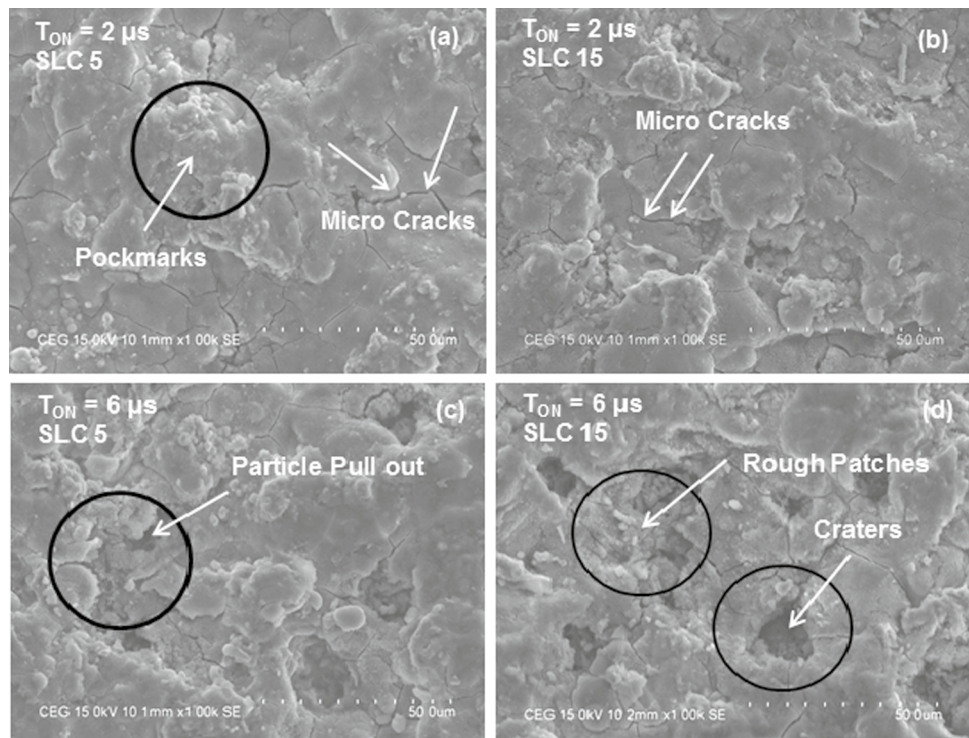
Figure 13 shows a substantial reduction in surface roughness caused by longer pulses-off duration, as a result of low material removal, and time is available for better flushing between inter-electrode gaps.

At shorter pulse-off duration, SLC 5 composite, B₄C particles expelled in addition to visible aluminum matrix melting layer, as shown in Fig. 14a. In the case of SLC 15, the possibility of reinforcement particles broken was very high, leading to the uneven surface and subsurface damage, as shown in Fig. 14b. On the other hand, for SLC 5, a longer pulse-off duration produced a slim melt layer resulting in a smoother machined surface as shown in Fig. 14c. For SLC 15 composite, reinforcement particles were slightly protruded from the machined surface, as shown in Fig. 14d.

Figure 15 shows the surface roughness variations in the composites with wire feed rates. A higher wire feed rate was preferred for SLC considering its offer of a low order of surface roughness. However, there was a slight increase in the surface roughness once it exceeds 8 mm/min. This could be due to the presence of a melt deposition layer between the inter-electrode gaps.

At a low wire feed rate, there was a continuous discharge of sparks at the same location. These eroded the metal along

Fig. 10 a–d SEM images of machined composites at different T_{ON}



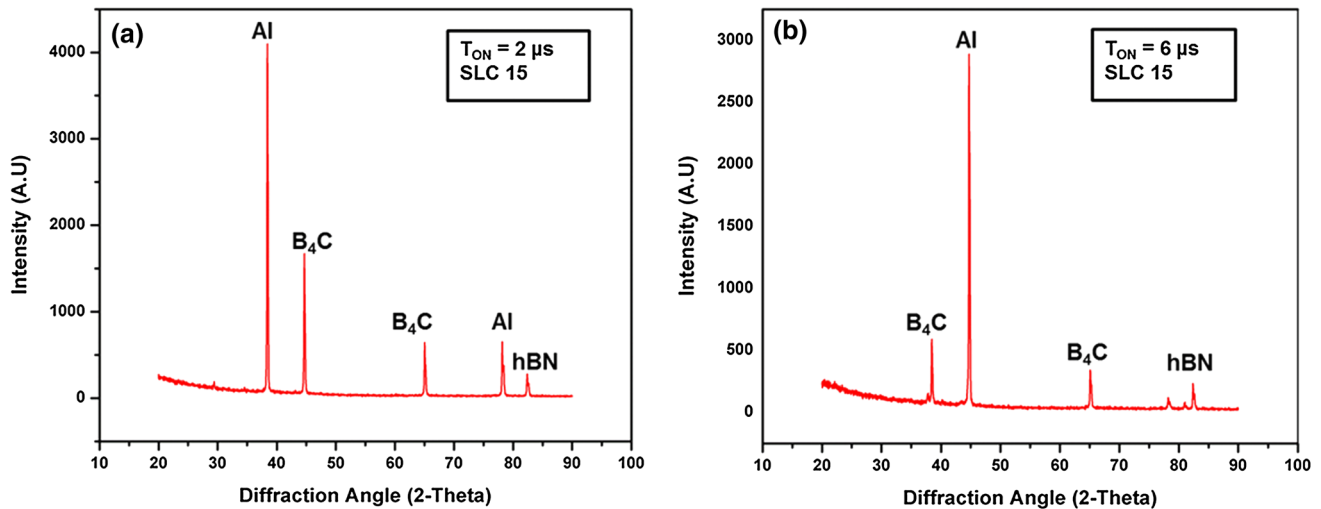
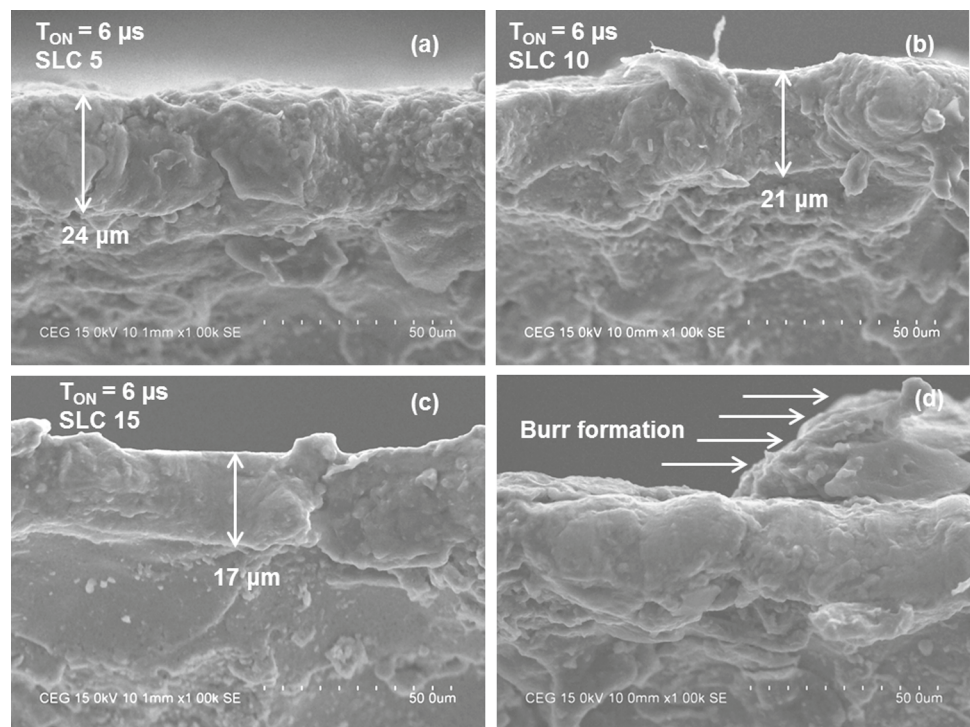


Fig. 11 a, b XRD pattern of machined composites at different T_{ON}

Fig. 12 a–d Recast layer of machined composites at maximum T_{ON}



with smaller-sized hBN particles from an SLC 5 composite, as shown in Fig. 16a. Similarly, in the SLC 15 composite, the metal matrix and reinforcement particles were subjected to severe thermal loading. This causes larger size craters, cracks, and voids, as shown in Fig. 16b. These defects had a severe effect on the surface roughness of the machined surface.

A higher wire feed rate placed limits on the electrical discharge interaction period with the material. This was evident from the SLC 5 composite, melting of the surface layer with

smaller droplets on the cut surface, as shown in Fig. 16c. Figure 16d shows an uneven topsy-turvy surface observed in the SLC 15.

Figure 17 shows the surface roughness variations in the composite with gap voltages. A higher gap voltage produces enormous discharge energy in the inter-electrode gap. It can be seen that the surface roughness of the machined surface increases with increasing gap voltage.

A large amount of melting of metal took place for the SLC 5 composites. This can be seen from Fig. 18a

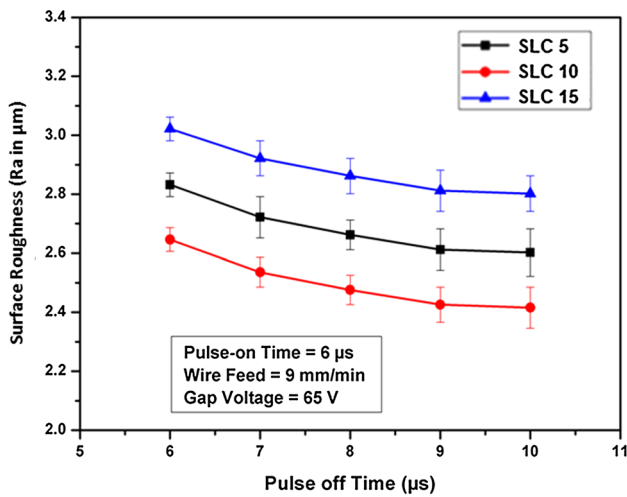


Fig. 13 Analysis of surface roughness by pulse-off time

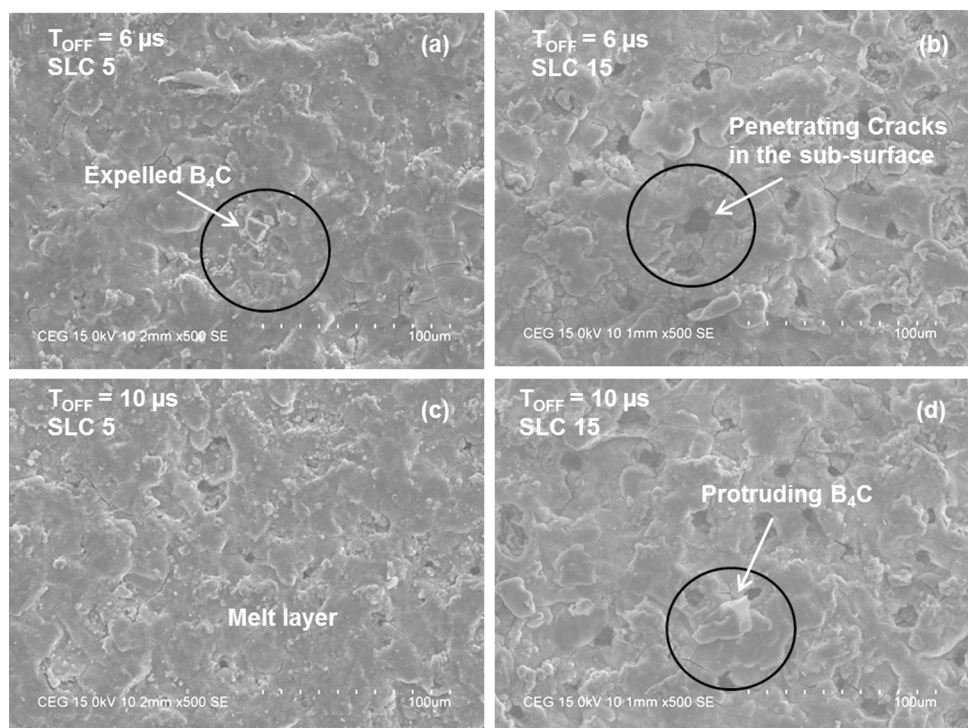
as a regular patch of the melted layer. When there was an increase in non-conductive hard B_4C particles in the matrix, SLC 15 composite could cause considerable impediment to the molten metal flow in the machining surface. Hence, irregular patches of the re-deposition layer were formed affecting surface roughness, as shown in Fig. 18b.

3.4 Triangular Corner Inaccuracy

Corner area inaccuracy from the triangular cut is measured for all three SLC composites. A typical triangular profile cutting is shown in Fig. 19. The WEDM parameters, namely pulse-on time and wire feed rate, are crucial for a proper corner cutting of composite materials. The above-mentioned two parameters were considered for triangular profile cutting, while other process parameters were kept constant. The deflection of the wire electrode due to flushing and dynamic forces by the discharge spark are also the reasons for corner inaccuracy [43]; this is not considered in this work.

Figure 20 depicts variations in corner area inaccuracy of the machined composites with pulse-on duration parameter. The electrical spark discharge does not have sufficient energy at a short pulse-on time to enable machining of all the sides of a corner for the composites studied. Then it leaves with a small area as un-machined, as shown in Fig. 21a, b. This problem compounded when machining of SLC 15 composite with a short pulse-on time. Hence, the corner area deviation is higher. Conversely, a longer pulse-on duration, especially in SLC 5 composite, produces a heavy melting of both sides of the corner material and subsequent re-deposition layer formation [44]. Finally, it ends up with increased dimensional corner area deviation. Further, an increase in reinforcement particles in the matrix, at longer pulse discharge

Fig. 14 a–d SEM images of machined composites at different T_{OFF}



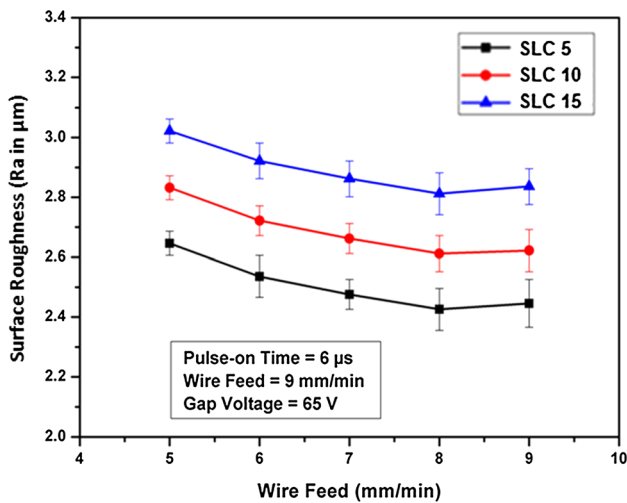


Fig. 15 Analysis of surface roughness by wire feed

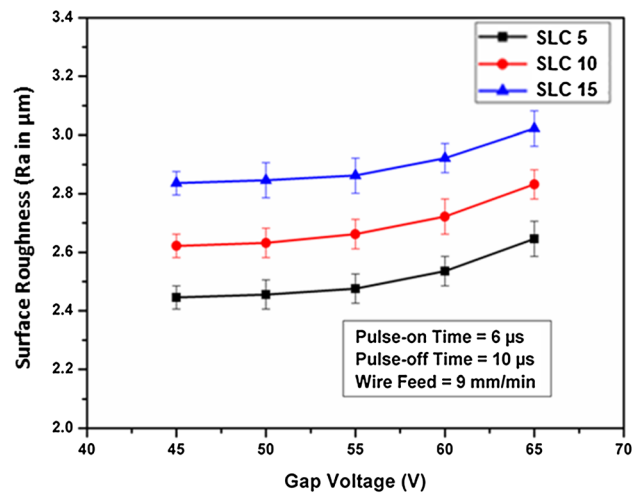


Fig. 17 Analysis of surface roughness by gap voltage

energy, reduces corner area deviation. Due to the erosion of aluminum, the metal cutting continued steadily at the corner area of the triangle profile. A high corner inaccuracy at a longer pulse-on duration could be seen. This could be due to an increase in the inter-electrode gap and frequency of wire break down caused by the wire electrode wear, as shown in Fig. 21c, d.

The variations in corner area inaccuracy with the wire feed rate are shown in Fig. 22. It can be seen that a corner with a dimensional inaccuracy decreases with wire feed rate. An inter-gap between the fast-moving wire electrode and the stationary workpiece was maintaining almost a setting value. Conversely, at a slow wire feed rate, the inter-electrode gap was largely affected. Continuous spark discharge at

Fig. 16 a–d SEM images of machined composites at different wire feeds

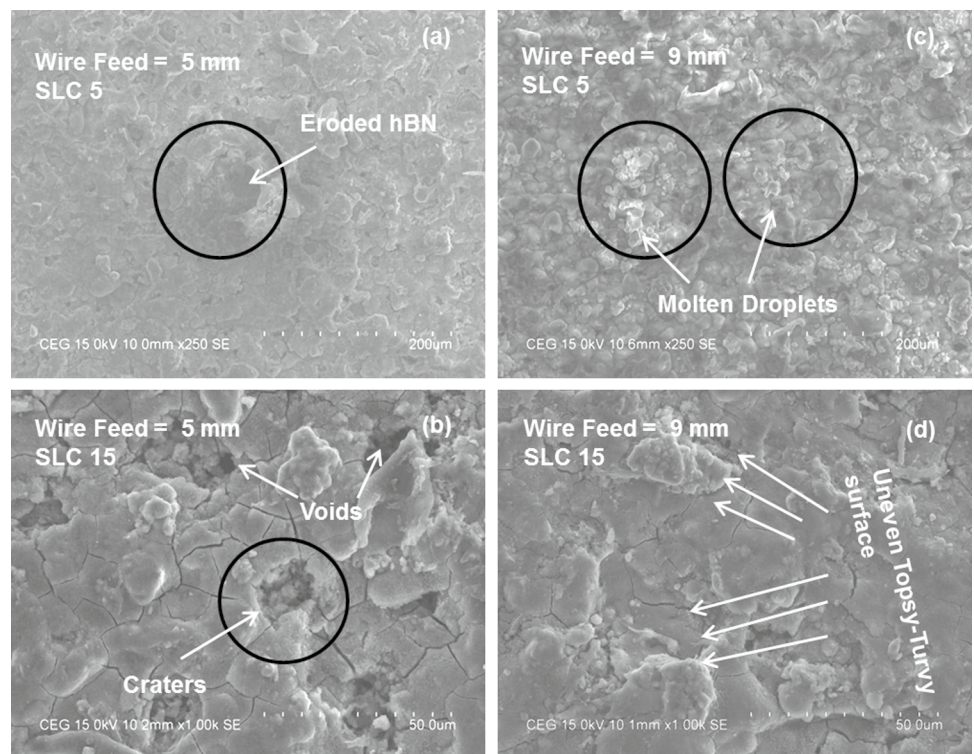


Fig. 18 a, b SEM images of machined composites at maximum gap voltage

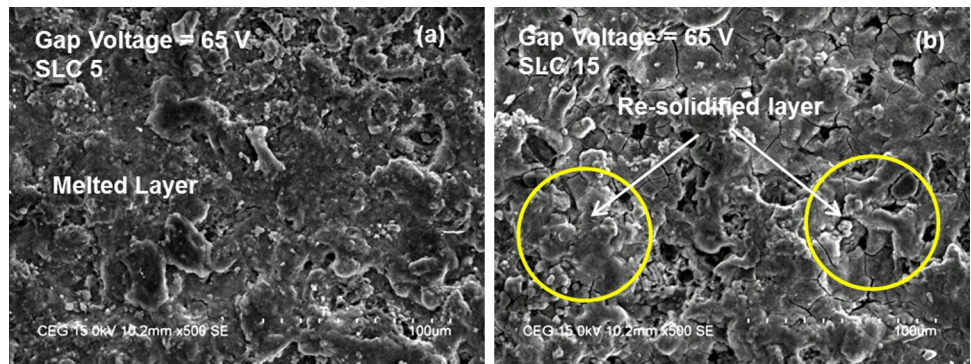


Fig. 19 Typical triangular profile cut

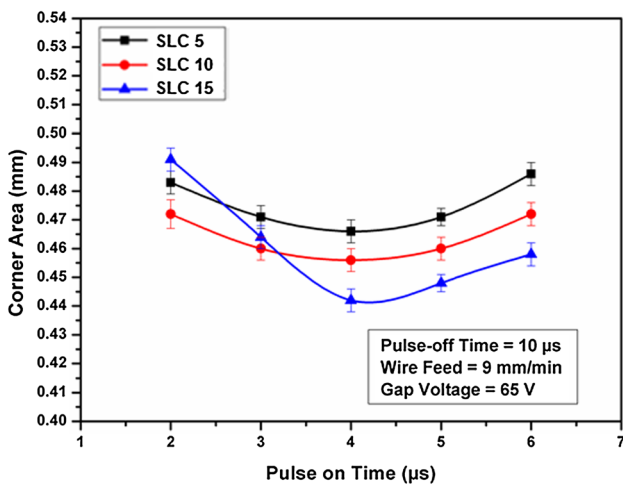
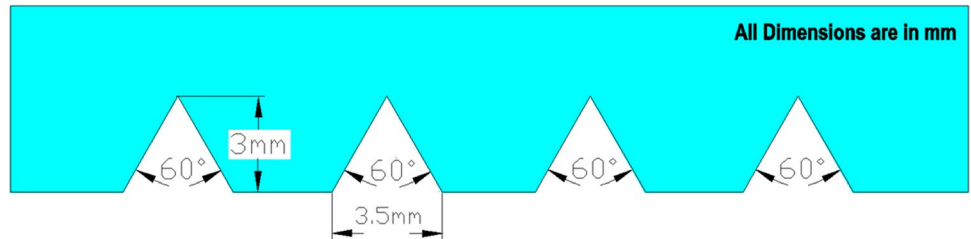


Fig. 20 Analysis of corner area by pulse-on time

a point could erode material of a large quantity. This causes an increase in an inter-electrode gap with corner area inaccuracy going up.

Corner area accuracy is affected with reinforcement particles which are located at the sharp corner made an ineffective cutting by wire electrode. This was due to the

shorter inter-distance between the particles and constriction imposed by fragmented B₄C and hBN particles deviating from the programmed path. Figure 23a–d clearly shows the corner inaccuracy as smaller in the higher feed rate than that of lower feed rate.

4 Conclusions

Wire cut electrical discharge with straight and triangular profile machining on the self-lubricating composite (SLC) was undertaken. The kerf dimensional deviation, surface characteristics, and corner area inaccuracy were studied with the effect of the spatial distribution of solid lubricant and boron carbide particles. The important conclusions are given below: SLC with 5%B₄C exhibits a larger kerf dimensional deviation due to rapid melting and evaporation of aluminum matrix. Further, an increase in B₄C particles reduces kerf dimensional deviation. It is of interest to note that a longer pulse-off duration reduces material removal, which is further reduced with an increase in B₄C content and the presence of hBN particles.

The prolonged energy discharges at low wire feed rate produce a wider kerf width dimension. The gap voltage with

Fig. 21 a–d Effect of pulse-on time on deviated corner area by triangular profile

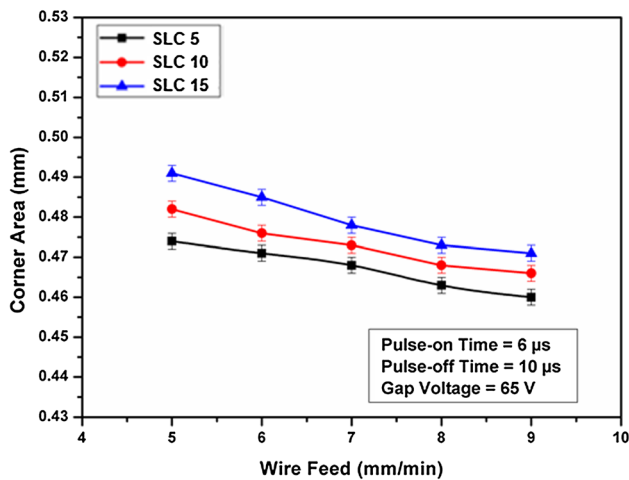
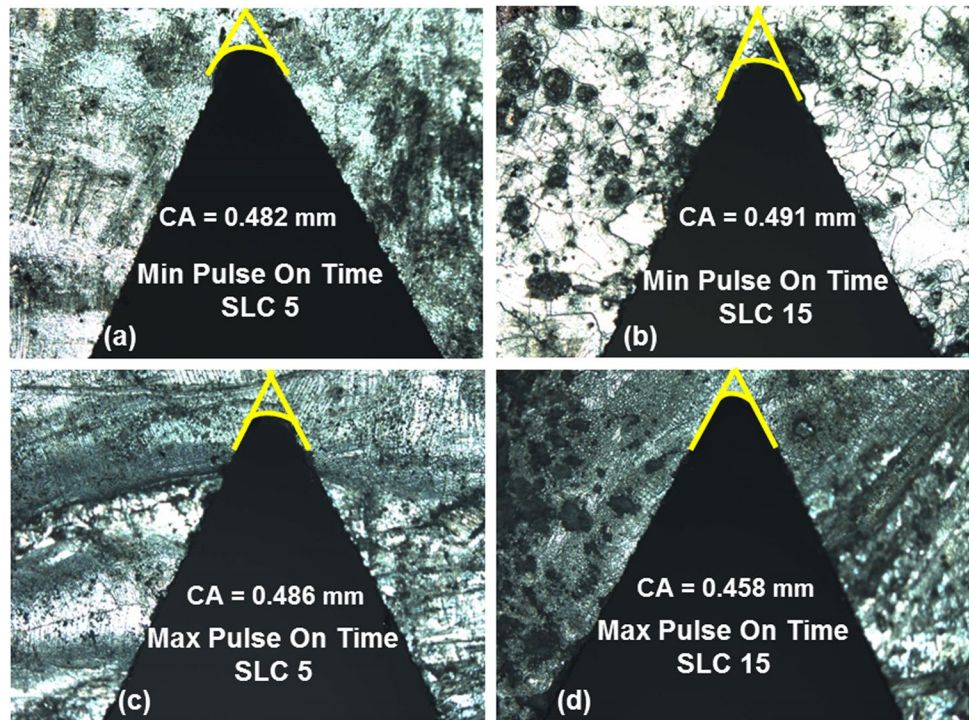


Fig. 22 Analysis of corner area inaccuracy by wire feed

high spark energy increases kerf width of 5% SLC, but the results reversed with increasing in B_4C particles.

Surface roughness of SLCs increases with a pulse-on duration due to larger material removal. This happens due to the presence of craters and pits on the cutting surface. 5 & 15% SLCs were characterized by depicting a poor surface

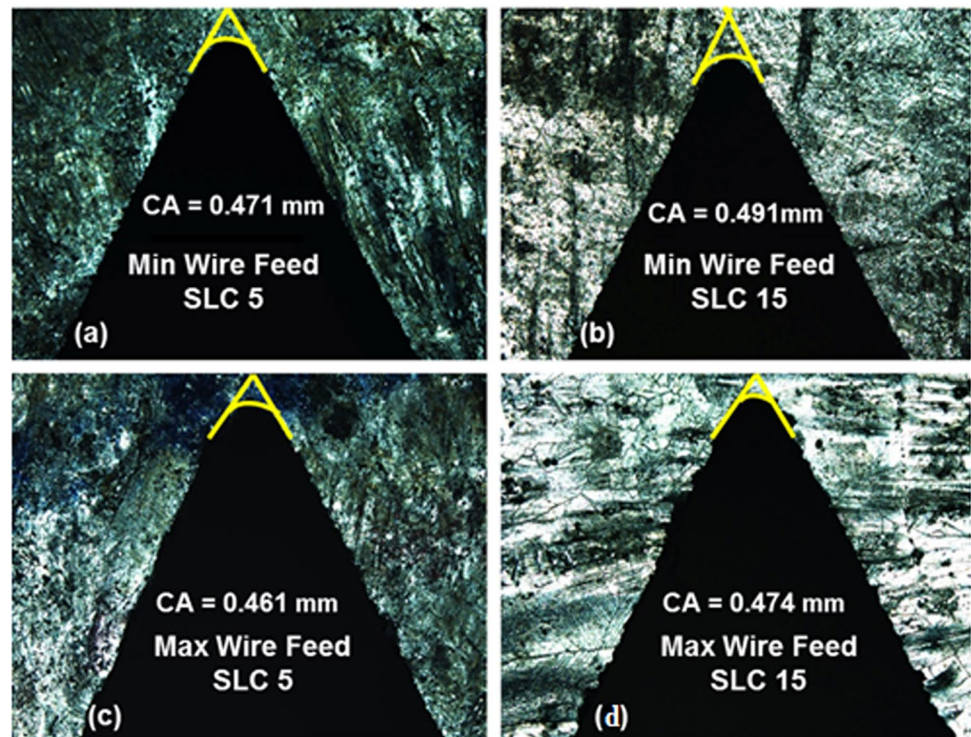
roughness due to the re-deposition layer and protrusion of B_4C particles. An increase in pulse-off duration, better flushing between the inter-electrode gap, and lower machining order resulted in a smoother surface.

At low wire feed rate and high gap voltage, SEM images of SLC machined surfaces reveal a solidified melted layer. Melted splash and blisters in this layer are indicators of high surface roughness. A higher wire feed rate preferred for SLC with relatively smoother cutting surfaces.

Corner area inaccuracy of triangular cut for all the three SLC reduces with a pulse-on duration. This is seen only up to $4 \mu s$, above which it begins to increase. This is the result of the heavy melting of the material, followed by a re-deposition layer at the triangle.

Experimental results reveal an increase in wire feed rate causing a decrease in the corner area inaccuracy of SLCs. This is the outcome of an almost constant inter-electrode gap between the fast-moving wire electrode and the stationary workpiece.

Fig. 23 a–d Effect of wire feed on deviated corner area by triangular profile



Acknowledgements The authors would like to express their sincere thanks to the Science and Engineering Research Board (SERB), Government of India, New Delhi, for providing the financial assistance for conducting this research through a Research Grant No. EEQ/2017/000382.

References

- Altan, T., Lilly, B.W., Kruth, J.P., Konig, W., Tonshoff, H.K., Van Luttervelt, C.A., Khairy, A.B.: Advanced techniques for die and mold manufacturing. *CIRP Ann.* **42**(2), 707–716 (1993)
- Ayoola, W.A., Adeosun, S.O., Sanni, O.S., Oyetunji, A.: Effect of casting mould on mechanical properties of 6063 aluminium alloy. *J. Eng. Sci. Technol.* **7**(1), 89–96 (2012)
- Chawla, K.K.: *Handbook on Composite Materials Science and Engineering*. Springer, Newyork (2001)
- Surappa, M.K.: Aluminium matrix composites: challenges and opportunities. *Sadhana* **28**(1–2), 319–334 (2003)
- Zhai, W., Shi, X., Wang, M., Xu, Z., Yao, J., Song, S., Wang, Y.: Grain refinement: a mechanism for graphene nanoplatelets to reduce friction and wear of Ni3Al matrix self-lubricating composites. *Wear* **310**(1–2), 33–40 (2014)
- Rajkumar, K., Gnanavelbabu, A., Venkatesan, M.S., Rajagopalan, K.: Cooperating function of graphite in reducing frictional wear of aluminium boron carbide composite. *Mater. Today Proc.* **5**(14), 27801–27809 (2018)
- Thangarasu, A., Murugan, N., Dinaharan, I., Vijay, S.J.: Synthesis and characterization of titanium carbide particulate reinforced AA6082 aluminium alloy composites via friction stir processing. *Arch. Civ. Mech. Eng.* **15**(2), 324–334 (2015)
- Walczak, M., Pieniak, D., Zwierchowski, M.: The tribological characteristics of SiC particle reinforced aluminium composites. *Arch. Civ. Mech. Eng.* **15**(1), 116–123 (2015)
- Ruirui, W., Zheng, Y., Qiushu, L.: Microstructure and mechanical properties of 7075 Al alloy based composites with Al₂O₃ nanoparticles. *Int. J. Cast Met. Res.* **30**(6), 337–340 (2017)
- Tan, A., Teng, J., Zeng, X., Fu, D., Zhang, H.: Fabrication of aluminium matrix hybrid composites reinforced with SiC micro particles and TiB₂ nano particles by powder metallurgy. *Powder Metall.* **60**(1), 66–72 (2017)
- He, D., Shang, L., Lu, Z., Zhang, G., Wang, L., Xue, Q.: Tailoring the mechanical and tribological properties of B4C/aC coatings by controlling the boron carbide content. *Surf. Coat. Technol.* **329**, 11–18 (2017)
- Loganathan, P., Gnanavelbabu, A., Rajkumar, K.: Analysis and characterization of friction behaviour on AA7075/ZrB₂ composite under dry sliding condition. *Mat. Res. Expr.* **6**(2), 026576 (2018)
- Duan, X., Yang, Z., Chen, L., Tian, Z., Cai, D., Wang, Y., Zhou, Y.: Review on the properties of hexagonal boron nitride matrix composite ceramics. *J. Eur. Ceram. Soc.* **36**(15), 3725–3737 (2016)
- Dai, S., Fei, Z., Ma, Q., Rodin, A.S., Wagner, M., McLeod, A.S., Taniguchi, T.: Tunable phonon polaritons in atomically thin van der Waals crystals of boron nitride. *Science* **343**(6175), 1125–1129 (2014)
- Chen, B., Bi, Q., Yang, J., Xia, Y., Hao, J.: Tribological properties of solid lubricants (graphite, hBN) for Cu-based P/M friction composites. *Tribol. Int.* **41**(12), 1145–1152 (2008)
- Pramanik, A.: Developments in the non-traditional machining of particle reinforced metal matrix composites. *Int. J. Mach. Tool. Manuf.* **86**, 44–61 (2014)
- Kozak, J., Rajurkar, K.P., Chandarana, N.: Machining of low electrical conductive materials by wire electrical discharge machining (WEDM). *J. Mater. Process. Technol.* **149**(1–3), 266–271 (2004)
- Zhang, C.: Effect of wire electrical discharge machining (WEDM) parameters on surface integrity of nanocomposite ceramics. *Ceram. Int.* **40**(7), 9657–9662 (2014)



19. Sarkar, S., Sekh, M., Mitra, S., Bhattacharyya, B.: A novel method of determination of wire lag for enhanced profile accuracy in WEDM. *Precis. Eng.* **35**(2), 339–347 (2011)
20. Shandilya, P., Jain, P.K., Jain, N.K.: Prediction of surface roughness during wire electrical discharge machining of SiCp/6061 Al metal matrix composite. *Int. J. Ind. Syst. Eng.* **12**(3), 301–315 (2012)
21. Ekici, E., Motorcu, A.R., Kuş, A.: Evaluation of surface roughness and material removal rate in the wire electrical discharge machining of Al/B4C composites via the Taguchi method. *J. Compos. Mater.* **50**(18), 2575–2586 (2016)
22. Ramesh, S., Natarajan, N., Krishnaraj, V.: Experimental investigation of Al6061/SiC p/B₄Cp hybrid MMCs in wire electrical discharge machine. *Indian J. Eng. Mater. Sci.* **21**, 409–417 (2014)
23. Pramanik, A., Littlefair, G.: Wire EDM mechanism of MMCs with the variation of reinforced particle size. *Mater. Manuf. Process.* **31**(13), 1700–1708 (2016)
24. Manna, A., Bhattacharyya, B.: Taguchi and Gauss elimination method: a dual response approach for parametric optimization of CNC wire cut EDM of PRAISiCMMC. *Int. J. Adv. Manuf. Technol.* **28**(1–2), 67–75 (2006)
25. Yan, B.H., Tsai, H.C., Huang, F.Y., Lee, L.C.: Examination of wire electrical discharge machining of Al₂O₃p/6061Al composites. *Int. J. Mach. Tool. Manuf.* **45**(3), 251–259 (2005)
26. Motorcu, A.R., Ekici, E., Kuş, A.: Investigation of the WEDM of Al/B4C/Gr reinforced hybrid composites using the Taguchi method and response surface methodology. *Sci. Eng. Compos. Mater.* **23**(4), 435–445 (2016)
27. Kandpal, B.C., Kumar, J., Singh, H.: Investigations into electrical discharge machining of fabricated AA 6061/10% Al₂O₃ aluminium-based metal matrix composite using OFAT approach. *Int. J. Automot. Compos.* **3**(1), 29–43 (2017)
28. Garg, M.P., Sharma, A.: Examination of accuracy aspect in machining of ZrSiO₄p/6063 aluminium MMC using CNC wire electrical discharge machining. *Compos. Commun.* **6**, 6–10 (2017)
29. Sanchez, J.A., Rodil, J.L., Herrero, A., De Lacalle, L.L., Lamikiz, A.: On the influence of cutting speed limitation on the accuracy of wire-EDM corner-cutting. *J. Mater. Process. Technol.* **182**(1–3), 574–579 (2007)
30. Selvakumar, G., Sarkar, S., Mitra, S.: Experimental investigation on die corner accuracy for wire electrical discharge machining of Monel 400 alloy. *Proc. Inst. Mech. Eng. Pt. B J. Eng. Manuf.* **226**(10), 1694–1704 (2012)
31. Selvakumar, G., Jiju, K.B., Sarkar, S., Mitra, S.: Enhancing die corner accuracy through trim cut in WEDM. *Int. J. Adv. Manuf. Technol.* **83**(5–8), 791–803 (2016)
32. Gnanavelbabu, A., Rajkumar, K., Saravanan, P.: Investigation on the cutting quality characteristics of abrasive water jet machining of AA6061-B4C-hBN hybrid metal matrix composites. *Mater. Manuf. Process.* **33**(12), 1313–1323 (2018)
33. Satishkumar, D., Kanthababu, M., Vajjiravelu, V., Anburaj, R., Sundarrajan, N.T., Arul, H.: Investigation of wire electrical discharge machining characteristics of Al6063/SiCp composites. *Int. J. Adv. Manuf. Technol.* **56**(9–12), 975–986 (2011)
34. Karabulut, Ş., Karakoç, H., Çitak, R.: Influence of B4C particle reinforcement on mechanical and machining properties of Al6061/B4C composites. *Compos. B Eng.* **101**, 87–98 (2016)
35. Chen, H.S., Wang, W.X., Li, Y.L., Zhang, P., Nie, H.H., Wu, Q.C.: The design, microstructure and tensile properties of B4C particulate reinforced 6061Al neutron absorber composites. *J. Alloys Compd.* **632**, 23–29 (6061Al)
36. Harichandran, R., Selvakumar, N.: Effect of nano/micro B₄C particles on the mechanical properties of aluminium metal matrix composites fabricated by ultrasonic cavitation-assisted solidification process. *Arch. Civ. Mech. Eng.* **16**(1), 147–158 (2016)
37. Garg, R.K., Singh, K.K., Sachdeva, A., Sharma, V.S., Ojha, K., Singh, S.: Review of research work in sinking EDM and WEDM on metal matrix composite materials. *Int. J. Adv. Manuf. Technol.* **50**(5–8), 611–624 (2010)
38. Lee, S.H., Li, X.P.: Study of the effect of machining parameters on the machining characteristics in electrical discharge machining of tungsten carbide. *J. Mater. Process. Technol.* **115**(3), 344–358 (2001)
39. Patil, N.G., Brahmanekar, P.K.: Some studies into wire electrodischarge machining of alumina particulate-reinforced aluminium matrix composites. *Int. J. Adv. Manuf. Technol.* **48**(5–8), 537–555 (2010)
40. Liao, Y.S., Huang, J.T., Chen, Y.H.: A study to achieve a fine surface finish in Wire-EDM. *J. Mater. Process. Technol.* **149**(1–3), 165–171 (2004)
41. Karabulut, Ş., Gökmen, U., Karakoç, H., Kalkan, Ö.K., Çitak, R.: Experimental investigation of B₄C particulate reinforced Aluminium 6061 based composite material in Wire-Cut EDM. *Metalophys. Adv. Technol.* **37**(9), 1239–1251 (2015)
42. Karabulut, Ş.; Karakoç, H.; Çitak, R.: Effect of the B4C reinforcement ratio on surface roughness of Al6061 based metal matrix composite in wire-EDM machining. In: 8th International Conference on Mechanical and Aerospace Engineering (ICMAE). Prague, pp. 812–815 (2017)
43. Puri, A.B., Bhattacharyya, B.: An analysis and optimisation of the geometrical inaccuracy due to wire lag phenomenon in WEDM. *Int. J. Mach. Tool. Manuf.* **43**(2), 151–159 (2003)
44. Hsue, W.J., Liao, Y.S., Lu, S.S.: Fundamental geometry analysis of wire electrical discharge machining in corner cutting. *Int. J. Mach. Tool. Manuf.* **39**(4), 651–667 (1999)

